ELSEVIER

Journal of Atmospheric and Solar-Terrestrial Physics 69 (2007) 1775–1796

Journal of ATMOSPHERIC AND SOLAR-TERRESTRIAL PHYSICS

www.elsevier.com/locate/jastp

Statistical observations of spatial characteristics of Pi1B pulsations

J.L. Posch[a,*], M.J. Engebretson[a], S.B. Mende[b], H.U. Frey[b], R.L. Arnoldy[c], M.R. Lessard[c], L.J. Lanzerotti[d], J. Watermann[e], M.B. Moldwin[f], P.V. Ponomarenko[g]

[a]*Department of Physics, Augsburg College, Minneapolis, MN, USA*
[b]*Space Sciences Laboratory, University of California, Berkeley, CA, USA*
[c]*Space Science Center, University of New Hampshire, Durham, NH, USA*
[d]*Center for Solar-Terrestrial Research, New Jersey Institute of Technology, Newark, NJ, USA*
[e]*Danish Meteorological Institute, Copenhagen, Denmark*
[f]*Institute of Geophysics and Planetary Physics, UCLA, Los Angeles, CA, USA*
[g]*School of Mathematical and Physical Sciences, University of Newcastle, NSW, Australia*

Received 22 August 2006; received in revised form 26 July 2007; accepted 31 July 2007
Available online 17 August 2007

Abstract

We have examined the spatial and temporal correlation of high-latitude Pi1B and Pi2 pulsations, mid-latitude Pi2 pulsations, and auroral substorm onsets identified in the IMAGE far ultraviolet imager (FUV) data. Numerous search coil and fluxgate magnetometers at high latitudes (65–80° in Antarctica and Greenland) and mid-latitude fluxgate magnetometers are used. We find that Pi1B onset times agree well with onset times of intense isolated auroral substorms identified by the IMAGE FUV instrument: Pi1B onsets occurred within the 2 min cadence of the imager. For any given event, we find that Pi1B are localized to approximately 4 h of local time and 7° of magnetic latitude relative to the initial auroral brightening location as observed by IMAGE FUV. Not surprisingly, we also find that Pi1B pulsations occur typically between 2100 and 0200 MLT. Comparison to Pi2 records from these and other lower-latitude stations shows that in almost all cases Pi1B activity coincides within ±2 min with Pi2 activity. Power law fits showed that Pi1B amplitude fell off with distance$^{-2.9}$ for two strong events (i.e., similar to the r^{-3} falloff of the signal from a dipolar source), and only slightly more rapidly than the falloff of Pi2 activity ($d^{-2.8}$). Given the global nature of Pi2 pulsations versus the localized nature of Pi1B events in this study, we conclude that the mechanism that drives Pi1B pulsations is likely different from that responsible for Pi2 pulsations.

Keywords: Substorms; Auroral phenomena; MHD waves and instabilities; Magnetic storms and substorms

*Corresponding author. Tel.: +1 612 330 1040; fax: +1 612 330 1649.
E-mail addresses: posch@augsburg.edu (J.L. Posch), engebret@augsburg.edu (M.J. Engebretson), mende@ssl.berkeley.edu (S.B. Mende), hfrey@ssl.berkeley.edu (H.U. Frey), Roger.Arnoldy@unh.edu (R.L. Arnoldy), Marc.Lessard@unh.edu (M.R. Lessard), ljl@njit.edu (L.J. Lanzerotti), jfw@dmi.dk (J. Watermann), mmoldwin@igpp.ucla.edu (M.B. Moldwin), phpp@alinga.newcastle.edu.au (P.V. Ponomarenko).

1364-6826/$ - see front matter © 2007 Elsevier Ltd. All rights reserved.
doi:10.1016/j.jastp.2007.07.015

1. Introduction

Arnoldy et al. (1998) used Pi1 search coil magnetometer signatures from an array of automated geophysical observatories (AGOs) in Antarctica, along with manned sites in both hemispheres (South Pole, Antarctica; Sondrestromfjord, Greenland; and Iqaluit, Canada), covering magnetic latitudes from 68° to 80°, to investigate the time development of the ground magnetic signatures in the region where auroras rapidly move poleward during the expansive phase of substorms. An important component of this investigation was to look at simultaneous geosynchronous orbit GOES magnetometer data within a few tens of degrees longitude of the ground sites. This study showed the following: (1) Pi1B (burst) waves were seen in space associated with magnetic field dipolarizations on the nightside, while the PiC (more continuous) waves were not seen in space. (2) The lowest-latitude ground station recording Pi1B detected these waves riding on a strong and sudden westward electrojet signal, which was not evident at the higher-latitude stations. (3) The higher-latitude stations saw a maximum Pi1B signal delayed consistent with auroral motion poleward. (4) There was a prompt Pi1B signal, which reached the higher-latitude stations, and even at other longitudes, whose onset seems to be related to the onset of the first evidence of Pi1B at low latitudes. This suggests horizontal ducting of waves from the field line of the onset station. (5) PiC across the entire Antarctic array seemed to be initiated by this same onset Pi1B signal. Finally, (6) ground Pi1 waves, particularly morning PiC, were closely associated with overhead particle precipitation for frequencies below 0.1 Hz. More recently, Lessard et al. (2006) presented observations from a case where Pi1B pulsations were seen on the ground, by GOES-9 at geosynchronous orbit, and also by FAST as it passed over the ground stations. Their analysis showed that the waves were compressional at GOES-9, but transverse as observed by FAST, suggesting that they propagated isotropically initially, but that they became guided as they approached lower altitudes.

The general association within a few minutes between substorm onset, auroral breakup, and onset of geomagnetic disturbance (bay, Pi2) is well established (e.g., Olson, 1999). Historically, significant emphasis has been placed on the importance of understanding the relative timing of various onset signatures, with hopes that the existence of a consistent ordering of events will lead to a better understanding of substorms. It now seems clear, however, that such an ordering may not exist or, perhaps, that ordering depends on the location of the observer (see, for example, the work by Arnoldy et al. (1998), where arrival times of Pi1B on the ground vs. by GOES are shown to depend on the relative positions in MLT). These results suggest that a more effective approach might be to understand the physical differences between the various signatures.

In addition to a "negative bay" at onset, which does appear to be well understood, there are two other magnetic signatures: Pi2 and Pi1B pulsations, neither of which is thoroughly understood. Pi2 pulsations are pulsations having periods between 40 and 150 s and have long been known to occur at substorm onset (Olson and Rostoker, 1978; Rostoker and Olson, 1978). While Kepko and Kivelson (1999) and Kepko et al. (2001) conclude that Pi2 pulsations result from the braking of fast flows associated with substorm onset, this conclusion has been questioned by Takahashi et al. (2001), who used CRRES data to show that this conjecture is not supported in their analysis, suggesting instead that a plasmaspheric cavity mode may be the source of the waves. On the other hand, Kim et al. (2005), examining another event, conclude that the observed frequency (11 mHz) is too low to be supported by a plasmaspheric cavity mode. Finally, Keiling et al. (2006) suggested that Pi2 pulsations (at least at high latitudes) are driven by pulsed reconnection in the plasmasheet that results in oscillating currents on the plasmasheet boundary layer.

While the mechanism responsible for Pi2 pulsations is not well understood, many observations show that these pulsations are often global in nature. In contrast, a main point of the work presented in this paper is that Pi1B pulsations are *not* global. This fact, combined with the fact that Pi1B pulsations are much higher in frequency (and have a distinct bursty nature), lead to a conclusion that Pi2 and Pi1B pulsations are not simply different perspectives of the same signature.

In this paper, we compare Pi1B signatures acquired from Antarctic stations with satellite images of substorm onsets. We also show corresponding Pi2 data acquired from Antarctic, Greenland, and North American sites. The focus of the case studies and statistical survey presented in this

paper is on spatial localization. Although Pi1B onset times agreed with onset times determined by the IMAGE FUV instrument to within its 2 min cadence, further consideration of the value of Pi1B from an array of stations for accurate timing of substorm onsets will be presented in a subsequent paper.

2. Instrumentation and data set

Automated Geophysical Observatories (AGOs) in Antarctica are operated by the United States (Rosenberg and Doolittle, 1994) and the United Kingdom (Dudeney et al., 1997). These AGOs include search coil magnetometers, which provide vector samples of dB/dt in local geomagnetic coordinates with X northward, Y eastward, and Z vertical (Taylor et al., 1975; Engebretson et al., 1997) at 0.5 s cadence. Similar search coil magnetometers at South Pole Station and McMurdo, Antarctica, provide vector samples at 0.1 s cadence. A fluxgate magnetometer, which provides data at one vector sample per second cadence, is also deployed at each of these sites. The combined Antarctic array covers geomagnetic latitudes from the auroral zone to the polar cap at geomagnetic longitudes from -33° to $+40^\circ$.

We have also used additional search coil data from Casey, Davis, and Mawson provided by the University of Newcastle. The geographic and geomagnetic coordinates of these stations, together with the sites of other stations used in this paper, are shown in Table 1. Fluxgate magnetometer data from the west coast of Greenland were supplied by the Danish Meteorological Institute (http://www.dmi.dk/projects/chain/greenland.html) and mid-latitude North American data (from the MEASURE array) were supplied by UCLA (http://measure.igpp.ucla.edu) (see Table 1). Stations along the west coast of Greenland are located near the magnetic longitude of AGO A81.

Fig. 1 shows a map of Antarctica with the stations used. The US AGOs are represented as open squares, the British AGOs as open triangles, and the Antarctic manned sites (South Pole, McMurdo, Casey, Davis, and Mawson) as solid circles. The conjugate locations of the Greenland sites are represented by an X and the four northernmost MEASURE sites (near the left-hand edge of the figure) by a +. The position of the substorm onset for each of the example events described in Section 3 is represented as an * and labeled with the corresponding day of year (DOY).

Table 1
Locations of the ground stations used in this study

Site	Geographic		Geomagnetic	
	Lat	Lon	Lat	Lon
Antarctica				
A80	−80.8	339.6	−66.5	28.5
A81	−81.5	3.0	−68.9	35.8
A84	−84.0	334.0	−70.0	25.0
AP1	−83.9	129.6	−80.1	16.8
AP2	−85.7	313.6	−69.8	19.2
AP3	−82.8	28.6	−71.8	40.2
AP5	−77.2	123.5	−86.7	29.4
SP	−90.0	0.0	−74.0	18.4
MC	−77.9	166.7	−79.9	326.8
CAS	−66.2	110.3	−80.8	153.6
MAW	−67.6	62.8	−70.3	89.5
DAV	−68.6	78.0	−74.5	103.0
Greenland				
THL	77.5	290.8	85.4	33.3
SVS	76.0	294.9	83.6	35.9
UPN	72.8	303.9	79.5	42.0
GDH	69.3	306.5	75.8	40.4
ATU	67.9	306.4	74.6	39.0
STF	67.0	309.3	73.2	41.7
GHB	64.2	308.3	70.6	38.5
FHB	62.0	310.3	68.0	39.7
NAQ	61.2	314.6	66.3	43.9
MCR	66.5	313.7	71.8	46.5
AMK	65.6	322.4	69.3	54.6
North American				
CLK	44.7	285.0	55.4	2.1
GFT	43.6	288.1	54.0	6.3
APL	39.1	283.1	50.21	358.8
DSO	36.3	278.6	47.6	352.1
FIT	28.1	279.0	39.6	352.1

The far ultra-violet imager (FUV) instrument is mounted on the IMAGE satellite, which is in a highly elliptical polar orbit of $1000 \times 45{,}600$ km altitude. The aurora is observed for 5–10 s during every 2 min spin period by the wideband imaging camera (WIC), one of three imaging subinstruments that make up the FUV system. The WIC has a passband of 140–180 nm, covering emissions from the N_2 LBH-band and atomic NI lines (Mende et al., 2000; Frey et al., 2004). Since the IMAGE satellite observes the aurora over the Northern Hemisphere and the search coil data used are from the Southern Hemisphere we must address hemispheric auroral asymmetries due to the clock angle (Østgaard et al., 2004, 2005). Fig. 1 of Østgaard

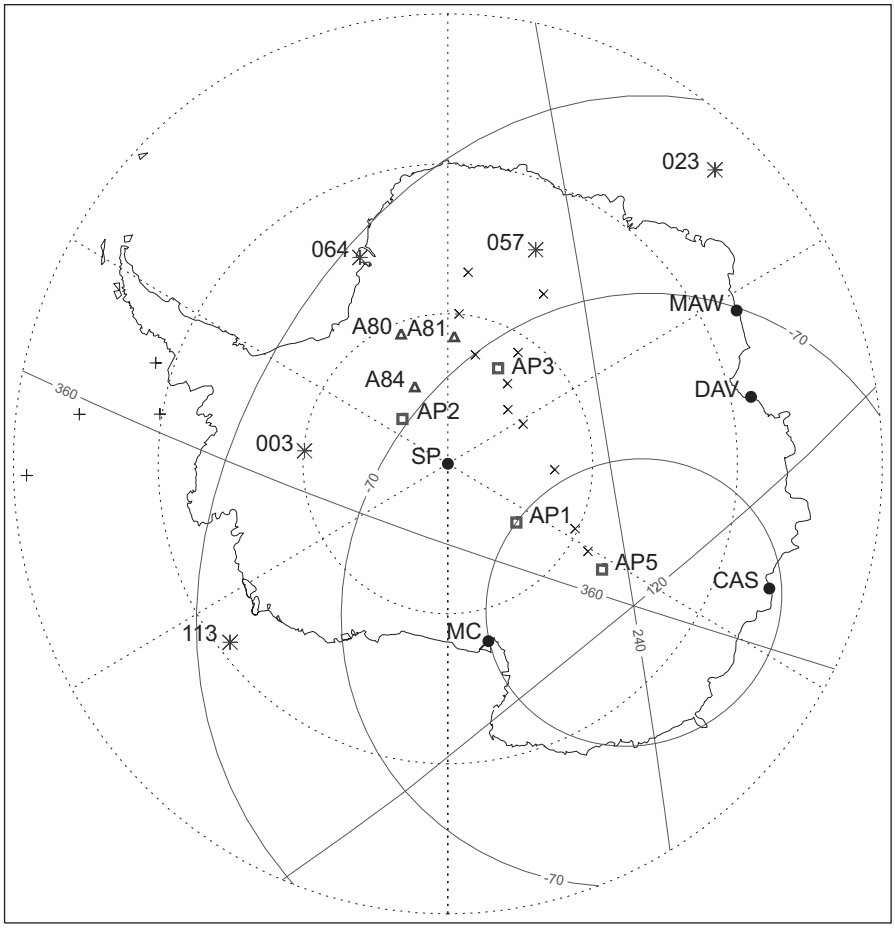

Fig. 1. Map of Antarctica showing locations of the Antarctic stations and conjugate locations of the Northern Hemisphere stations listed in Table 1. The position of the substorm onset for each of the example events is labeled with the corresponding DOY. Geographic latitude and longitude are indicated by dashed lines and geomagnetic by solid lines.

et al. (2005) quantifies the observed asymmetries and will be used to show the expected asymmetries for the several events, which are discussed in Section 6.

We began our study with a list of 112 substorm onsets identified at the University of California, Berkeley, from FUV-WIC imager data during the approximate 11-month interval from June 28, 2000 to June 2, 2001. Frey et al. (2004) identified a substorm onset when there was a clear local brightening of the aurora that expanded to the poleward boundary of the oval and spread azimuthally in local time for a minimum of 20 min. The substorm onset also had to occur at least 30 min after a previous onset.

Using the original list of 112 substorm onsets, we focused on the time interval of 20–06 UT, which corresponds roughly to local times from 17 to 03 MLT at the Antarctic stations. Limiting the study to this time interval reduced the original list of 112 to 39 onset events; these events will be referred to as the original 39 events from now on.

A new expanded list of substorm onsets covering May 16, 2000–December 31, 2002 (Frey et al., 2004) included 885 events during the original interval from June 28, 2000 to June 2, 2001. The original 39 events were verified to be on the new list, but the number of events in the correct time sector in this larger list was too extensive to include in this study. Instead, we included the 16 additional events from the new list occurring between 20 and 06 UT with greater than 10,000 counts (the raw instrument counts in the brightest pixel at substorm onset). This count level is equivalent to 16.3 kR using the conversion factor of 612.6 counts/kR (Frey et al., 2003). These 16 events, together with the 4 events

with brightness greater than 16.3 kR from the original list of 39, gave another set of 20 events with brightness greater than 16.3 kR for analysis during the June 28, 2000–June 2, 2001 interval. The brightness of the substorm onsets in the combined data set ranged from 3.9 to 30.1 kR.

For each of the events from both data sets, search coil data from all available Antarctic stations were analyzed for Pi1B pulsations. We produced differenced 0–1 Hz Fourier spectrograms of the x (North–South) component from the 0.5 s data using a 256-point FFT calculated every 20 points with a noise floor of approximately 10^{-6}–10^{-7} nT^2 Hz, covering 1 h around the observed onset time.

3. Example events

For each of the following events we show a sequence of 2 WIC images with the position of the Antarctic stations mapped onto them and a stacked 1-h Fourier spectrogram of Antarctic search coil magnetometer data. We also show stacked line plots of raw search coil data, filtered fluxgate magnetometer data from these same Antarctic stations, and filtered Pi2 data from the Western Greenland chain and from the MEASURE array in North America. For 2 events, search coil data from one or all of Casey, Davis, and Mawson will be shown. Three examples of good Pi1B indicators of substorm onset are shown first, and then two examples, for which Pi1B disturbances do not appear at these stations at the time of substorm onset. For each of the examples the parameters ΔMLAT, ΔMLT, and substorm onset brightness will be given. ΔMLAT is defined as the difference in degrees between the onset location identified in the WIC imager data and the reference magnetic latitude, which is within the auroral zone stations used in this study (negative ΔMLAT indicates that the reference latitude is equatorward of the onset location), ΔMLT is defined as the difference in hours between the onset location identified in the WIC imager data and the reference local time of the auroral zone stations used in this study (negative ΔMLT indicates that the reference local time is duskward of the onset location), and maximum brightness is given in kR. The reference local time is calculated using the time of the substorm onset and the average magnetic longitude of 31°, which corresponds to a local magnetic midnight of 3 UT. This average is approximated using the locations of A80, A81, A84, and SP, which are the stations where data were available most often. The reference magnetic latitude used was 67°, which was weighted toward the lower latitudes of the BAS AGO stations. Since the position of the substorm onset is given as a single-point position of the brightest pixel rather than as a range of latitudes and longitudes, it is reasonable to use a reference position for statistical purposes.

3.1. Substorm onsets with Pi1B activity

3.1.1. February 26, 2001, substorm onset = 1:23:27 UT

The substorm onset of February 26, 2001 (DOY 057) occurred at 1:23:27 UT with maximum brightness = 26.7 kR, ΔMLAT = 0.2, and ΔMLT = 1.6. The intense onset is seen in the WIC images shown in the left-hand panels of Fig. 2. The upper image was obtained at 1:21:24 UT, just prior to onset time, and the lower image shows the intense brightening that was recorded at 1:23:27 UT. The available Antarctic stations are mapped to their conjugate site on the WIC image, which is a view from the Northern Hemisphere with geomagnetic coordinates shown. The substorm onset brightening, which occurred at 66.8° MLAT and 24.0 MLT is closest in MLT to AGO A81 (Fig. 1). One-hour spectrograms starting at 1:00 UT of search coil magnetometer data from the 8 available stations are shown in the right-hand panel of Fig. 2 with the substorm onset time indicated by the red vertical line at 1:23:27 UT. The two white vertical lines on either side of the red are ±2 min from onset. Pi1B activity is strongest at A81 and is clearly evident at all 8 available sites, but it is much weaker at the 4 most distant stations, South Pole, McMurdo, Casey, and Davis. This is the most intense of the example "Yes" events shown in Section 3.1 of this paper and the only one with Pi1B activity at all stations.

Pi1B activity is also seen in Fig. 3A, which shows the 1-h time series of the Antarctic search coil data starting at 0100 UT, although it is not as clear at Casey. Fig. 3B shows 7–25 mHz band pass filtered fluxgate magnetometer data for many of the stations shown in Fig. 3A. These data show that Pi2 are occurring at the same time as the Pi1B in the search coil data. Fig. 3C shows 7–25 mHz band pass filtered fluxgate magnetometer data from the MEASURE array and Fig. 3D shows 3-min high pass filtered fluxgate data from the Greenland chain of fluxgate magnetometers. Clear Pi2 signals are

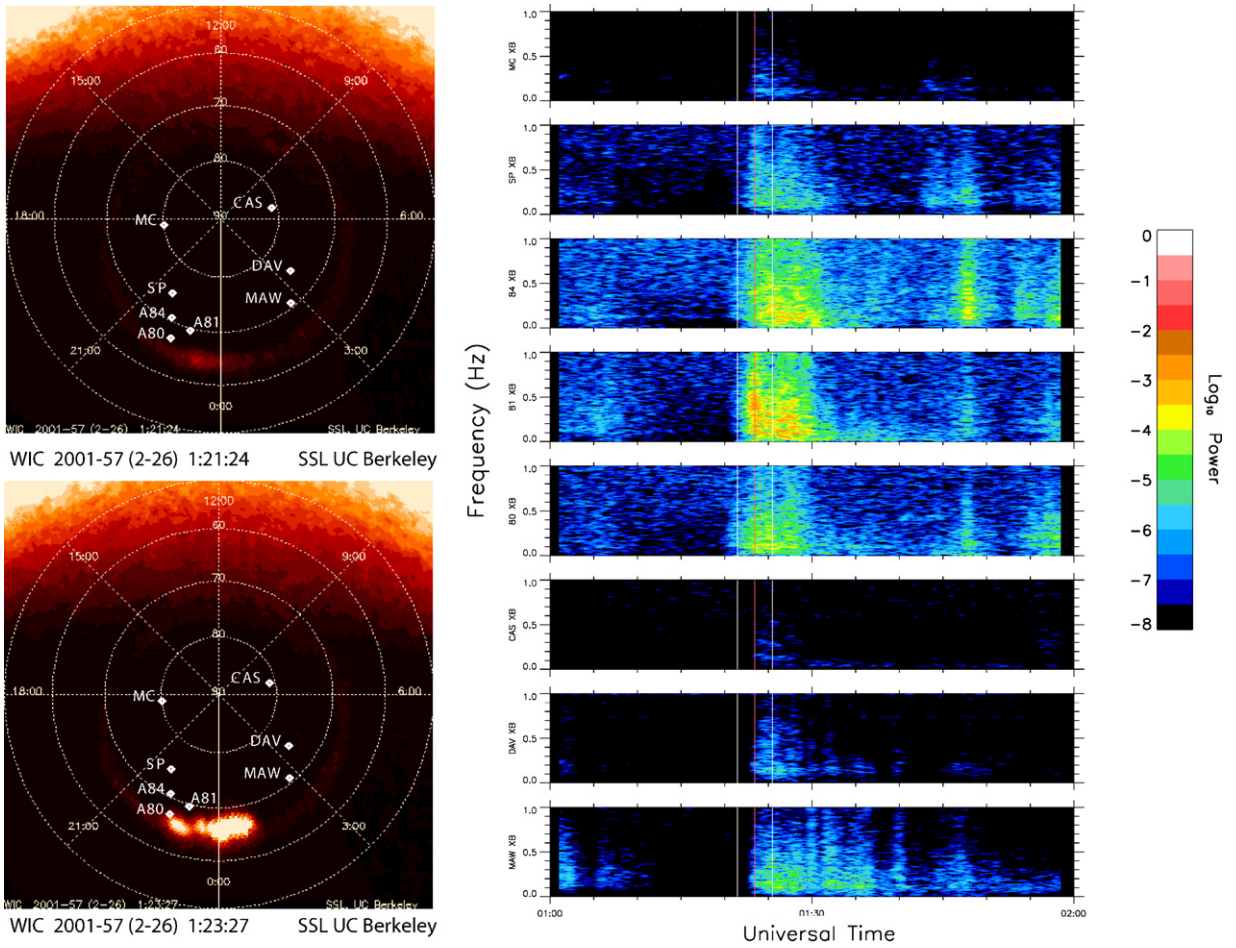

Fig. 2. The 2 panels on the left are WIC images showing the substorm onset of February 26, 2001 (DOY = 057), mapped onto a magnetic coordinate grid. The upper left panel shows the image preceding the onset and the lower left shows the time of onset. The positions of the Antarctic stations available for the event are mapped onto each of the WIC images. The right side of the figure shows a 1-h, 0–1 Hz Fourier spectrogram of search coil data from several Antarctic ground stations during this event. The vertical red line shows the time of substorm onset and the 2 vertical white lines show ±2 min of the onset time.

seen at the 4 available stations from MEASURE and several of the Greenland sites near the time of substorm onset, which is indicated by the vertical line shown in all panels.

3.1.2. *January 3, 2001, substorm onset = 2:35:11 UT*

Fig. 4 shows the substorm onset of January 3, 2001 (DOY 003), which occurred at 2:35:11 UT. In this case, the maximum brightness = 10.1 kR, ΔMLAT = 1.5, and ΔMLT = 1.6. The WIC images in the left-hand panels of Fig. 4 show a fairly weak onset covering a limited region centered at 65.5° MLAT and 22.0 MLT. As in Fig. 2, the upper WIC image is just prior to substorm onset and the lower shows the time of the substorm onset.

In this example, the 1-h spectrogram in the right panel starting at 2:00 UT shows 7 Antarctic

Fig. 3. Magnetometer data from several stations in Antarctica and the Northern Hemisphere for February 26, 2001. Panel A shows 1 h of *x*-component raw search coil (dB/dt) data from the Antarctic stations shown in the previous figure. Panel B shows 7–25 mHz band pass filtered data, North–South (H component) fluxgate magnetometer data, from these same stations where available. Panel C shows 7–25 mHz band-pass filtered data from the MEASURE array in North America. Panel D shows 3-min high pass filtered fluxgate data from the Greenland stations. The vertical lines in each panel indicate the substorm onset time.

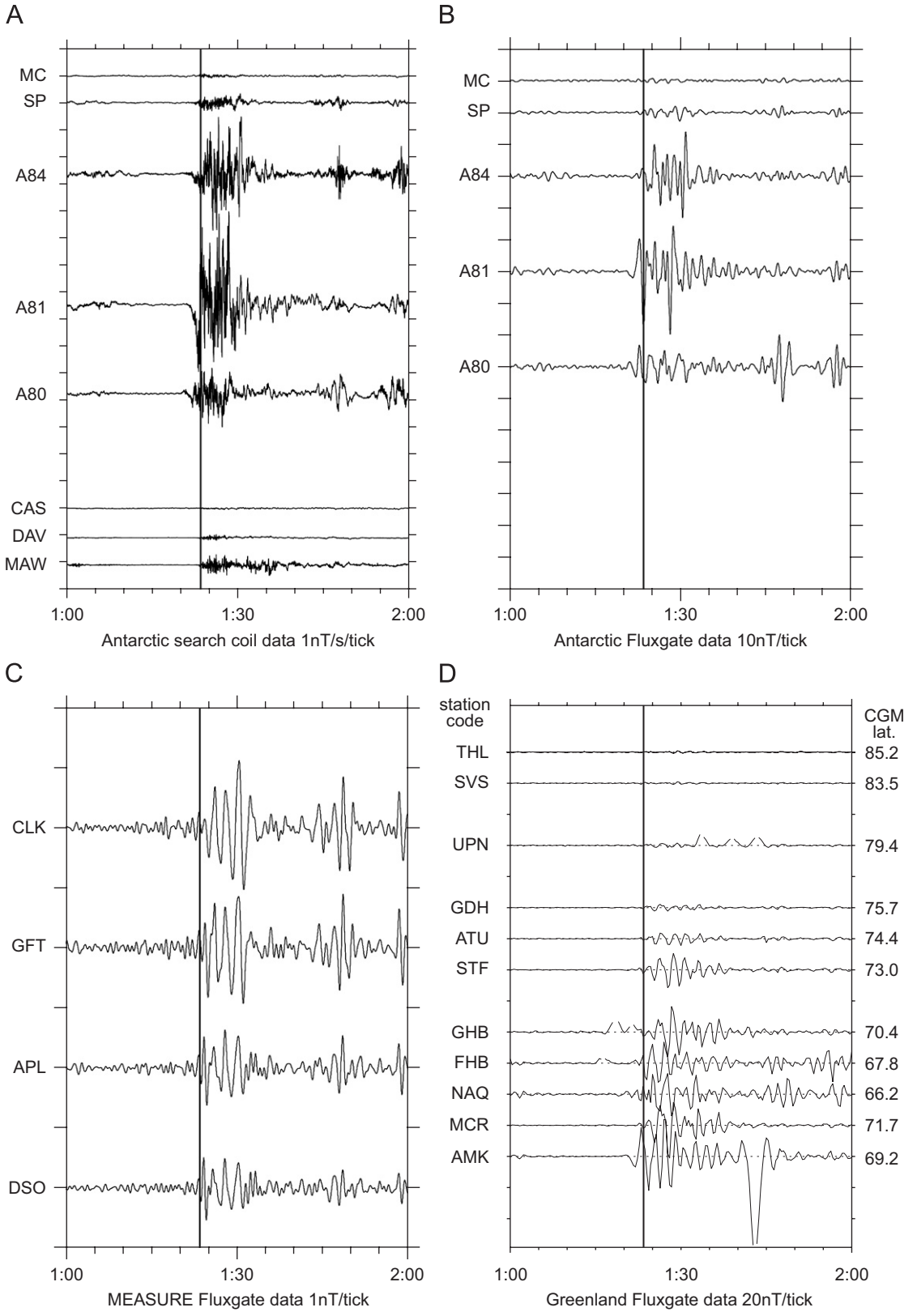
A
MC
SP
A84
A81
A80
CAS
DAV
MAW
1:00
1:30
2:00
Antarctic search coil data 1nT/s/tick
B
MC
SP
A84
A81
A80
1:00
1:30
2:00
Antarctic Fluxgate data 10nT/tick
C
CLK
GFT
APL
DSO
1:00
1:30
2:00
MEASURE Fluxgate data 1nT/tick
D
station code
CGM lat.
THL 85.2
SVS 83.5
UPN 79.4
GDH 75.7
ATU 74.4
STF 73.0
GHB 70.4
FHB 67.8
NAQ 66.2
MCR 71.7
AMK 69.2
1:00
1:30
2:00
Greenland Fluxgate data 20nT/tick

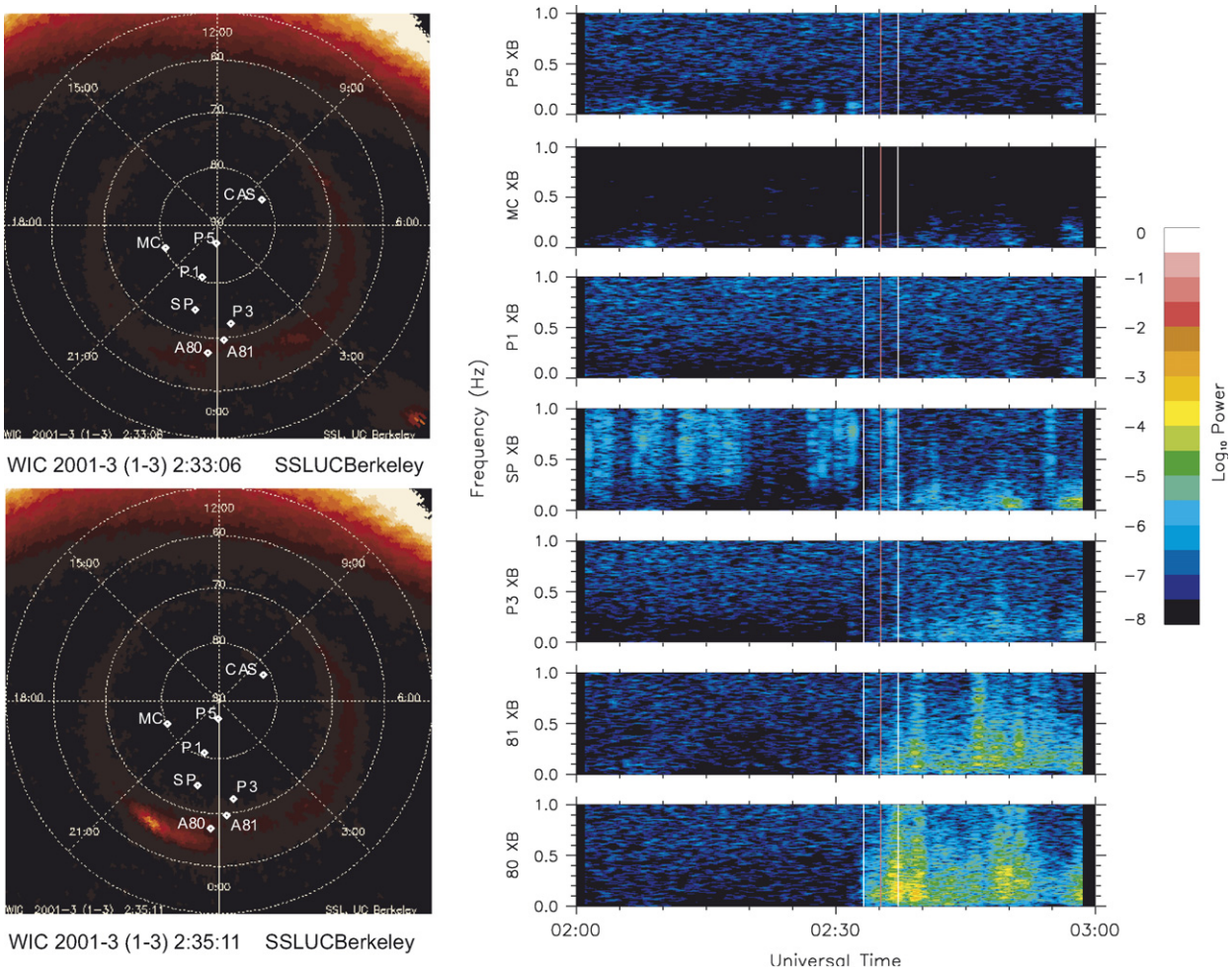

Fig. 4. The two panels on the left are the WIC images showing the substorm onset and the right side of the figure shows a 1-h, 0–1 Hz Fourier spectrogram of search coil data from several Antarctic ground stations as in Fig. 2, but for January 3, 2001 (DOY = 003).

stations. Clear Pi1B activity is seen at the 2 lowest-latitude stations, A80 and A81, and marginal Pi1B activity at P3 and South Pole. Casey data were also available for this event but did not show any Pi1B activity.

This example (Fig. 4) shows that South Pole station is closer in distance and MLT to the brightest point of the substorm onset than A81, but it is further in latitude from the substorm onset location—which is narrow in latitude but extends in longitude—bringing it much closer to A81. So in this case, in which South Pole does not have clear Pi1B activity but A81 does, the difference in latitude may be playing a more important role than the difference in MLT in limiting the occurrence of Pi1B.

The time series of search coil data for January 3, 2001 from 2:00 to 3:00 UT in Fig. 5A shows the clear onset of Pi1B activity near 2:35 UT at both A80 and A81. As in the spectrogram of Fig. 4, the time series plot of search coil data shows marginal Pi1B activity at P3 and South Pole and the higher-latitude stations do not show any Pi1B activity. The fluxgate magnetometer data from A80 and A81, shown in Fig. 5B, show a fairly clear but gradual increase of Pi2 activity corresponding to the substorm onset at 2:35 UT. The higher-latitude stations also show Pi2 around 2:35 UT, however, there are also Pi2-type wave bursts several minutes before and after this time. Pi2 activity can also be seen (shown in Fig. 5C and D) at the MEASURE stations and at the Greenland stations between 66.2° and 71.7°, but no signals are evident at higher-latitude stations. We also note that even though the WIC imager recorded a significantly weaker auroral

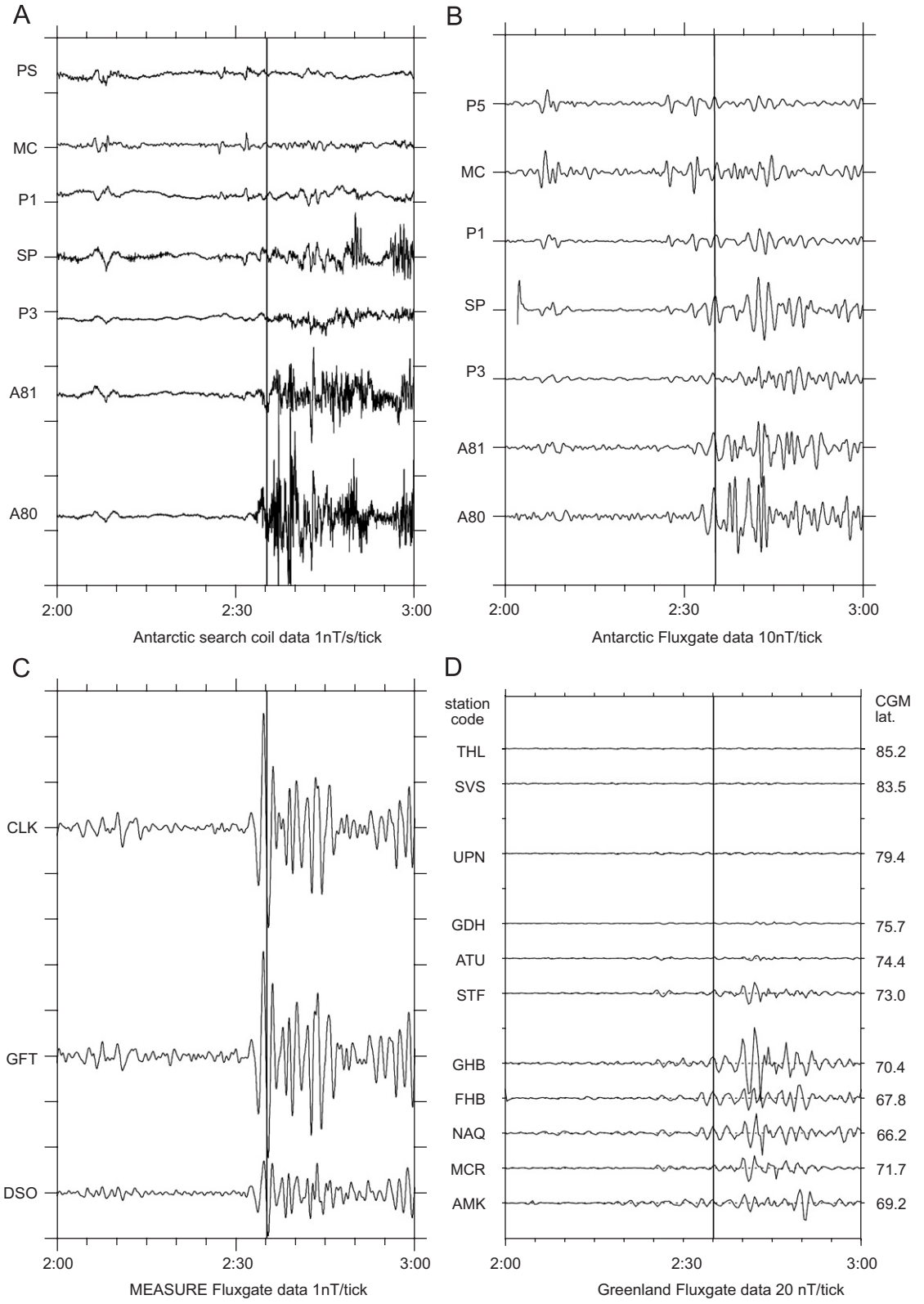

Fig. 5. Magnetometer data from several stations in Antarctica (A and B), North America (C), and Greenland (D) as in Fig. 3, but for January 3, 2001 (DOY = 003).

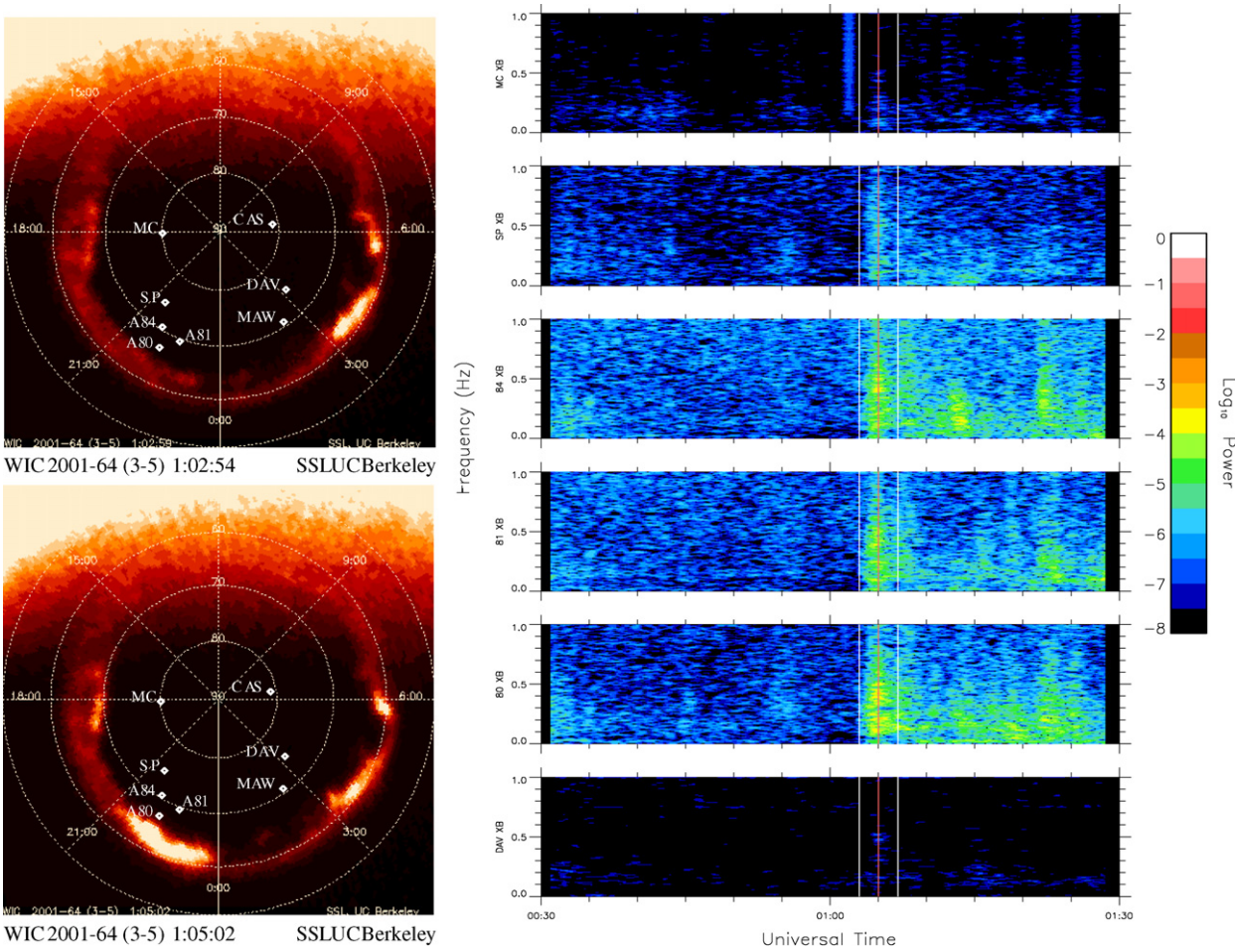

Fig. 6. The 2 panels on the left are the WIC images showing the substorm onset and the right side of the figure shows a 1-h, 0–1 Hz Fourier spectrogram of search coil data from several Antarctic ground stations as in Fig. 2, but for March 5, 2001 (DOY = 064).

brightening for this event, and Pi1B signals were correspondingly weak, the Pi2 signals were stronger at the low-latitude MEASURE stations for this event than for the event in Fig. 2.

3.1.3. March 5, 2001, substorm onset = 1:05:02 UT

A strong substorm onset with brightness = 22.0 kR occurred at 1:05:02 UT on March 5, 2001 (DOY = 064) at 61.7° MLAT and 22.1 MLT. The substorm onset, shown in the lower left panel of Fig. 6, was very close in longitude to all available stations (ΔMLT = 0.0), but occurred at a lower latitude (ΔMLAT = 5.3). Prior to substorm onset, the WIC recorded aurora over almost the entire night side oval. Emissions were especially strong in the interval between 0300 and 0600 LT. Such auroral activity produces significant local magnetic disturbances.

Pi1B activity is evident at each of the 6 sites shown, but, as can be seen in the 1-h spectrogram starting at 00:30 UT shown in the right panel of Fig. 6, it was very weak at McMurdo and Davis. No Pi1B activity was evident at Casey (not shown). Again, as in the first example, the station, which was closest to the substorm onset, in this example A80, had the most intense Pi1B activity. This is an excellent example of the Pi1B signal being clearly distinguishable above geomagnetic activity associated with the general auroral oval emissions.

Fig. 7A shows the search coil magnetometer time series data for this interval. A clear onset of Pi1B activity is evident at the 3 lowest latitude stations A80, A81, and A84. The Pi1B was not seen as clearly at the two higher-latitude stations, South Pole and McMurdo, but may be evident by the thickening of the trace. No such change is evident in

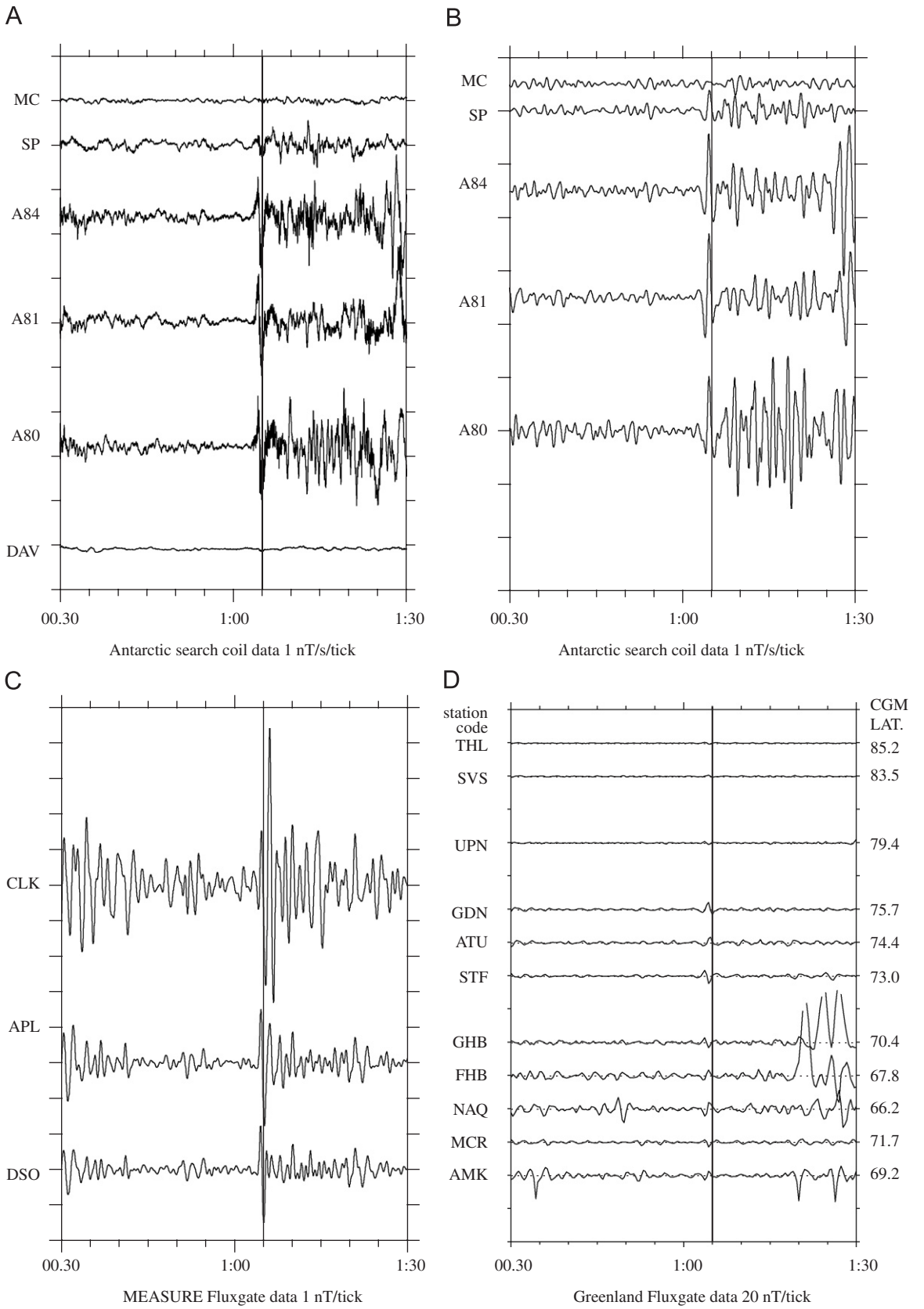

Fig. 7. Magnetometer data from several stations in Antarctica (A and B), North America (C), and Greenland (D) as in Fig. 3, but for March 5, 2001 (DOY = 064).

the trace at Davis. The Antarctic fluxgate data in Fig. 7B show a clear onset of Pi2 indicated by the large spike occurring about 1:05 UT at all sites except McMurdo, which was poleward of the auroral zone for this event. This spike occurs as well in the MEASURE fluxgate data shown in Fig. 7D. The Greenland magnetometer data in Fig. 7D show only a rather weak onset of Pi2 activity near the time of substorm onset, despite the nominal conjugacy of the stations in Western Greenland to the magnetic longitude of A81, as shown in Fig. 1. The intensity of Pi2 activity at the Greenland stations near 1:05 UT was in fact weaker than that which had occurred since intense substorm activity began on March 4 around 20 UT and had continued intermittently for several hours.

3.2. Substorm onsets without Pi1B activity

3.2.1. January 23, 2001, substorm onset = 22:26:20 UT

On January 23, 2001(DOY = 023) a substorm onset was identified at 22:26:20 UT in the WIC images as seen in the lower left panel of Fig. 8. The substorm onset was moderately strong with brightness = 16.0 kR but it covered a limited range centered at 63.3° MLAT and 22.8 MLT. The auroral oval was particularly active around almost the entire midnight to late morning sector.

The 4 available stations were fairly close in latitude with ΔMLAT = 3.7° but not close in local time, ΔMLT = −3.3. The spectrogram from 22:00 to 23:00 UT shown in the right panel of Fig. 8 shows that no Pi1B activity was seen within ±15 min of

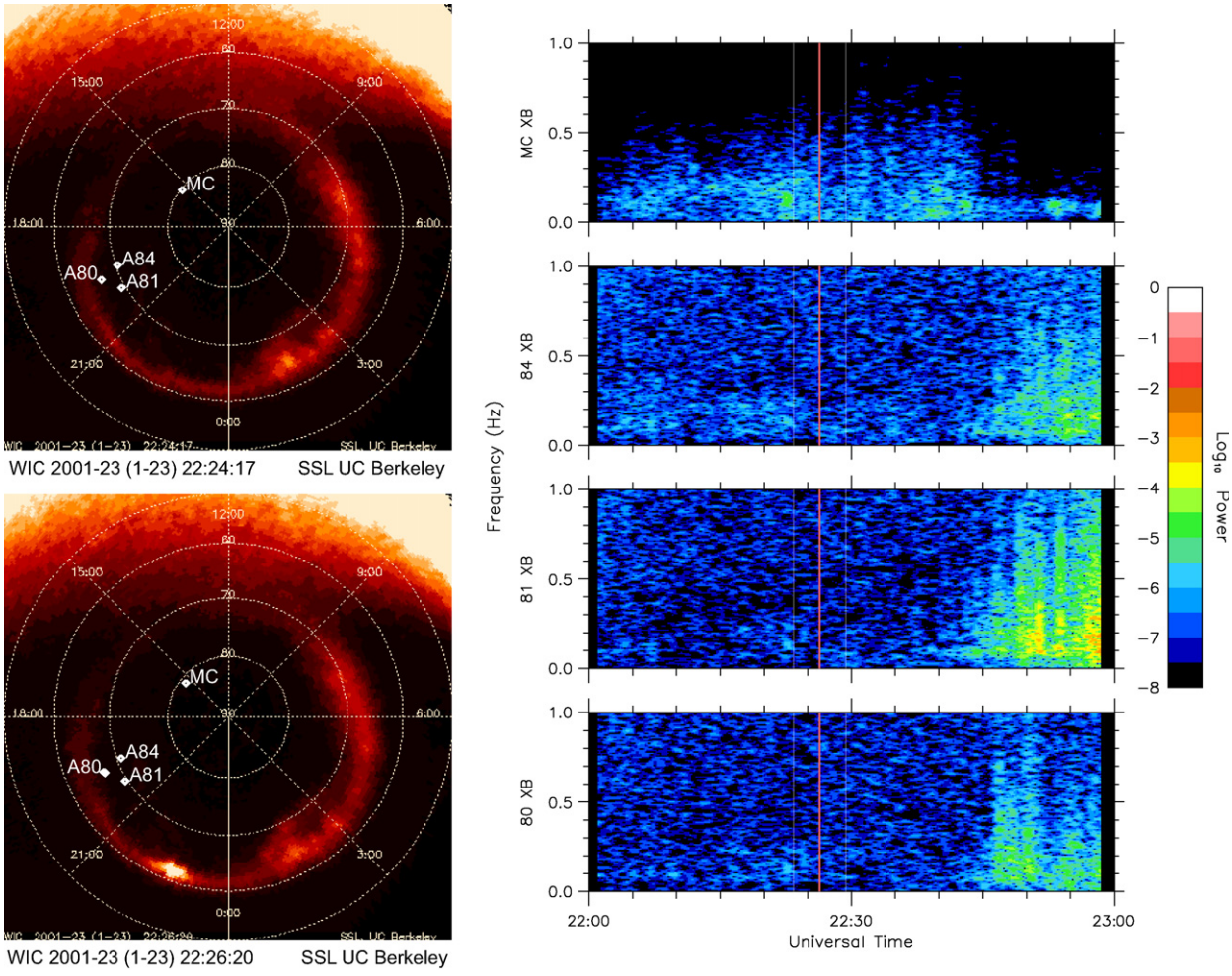

Fig. 8. The 2 panels on the left are the WIC images showing the substorm onset and the right side of the figure shows a 1-h, 0–1 Hz Fourier spectrogram of search coil data from several Antarctic ground stations as in Fig. 2, but for January 23, 2001 (DOY = 023).

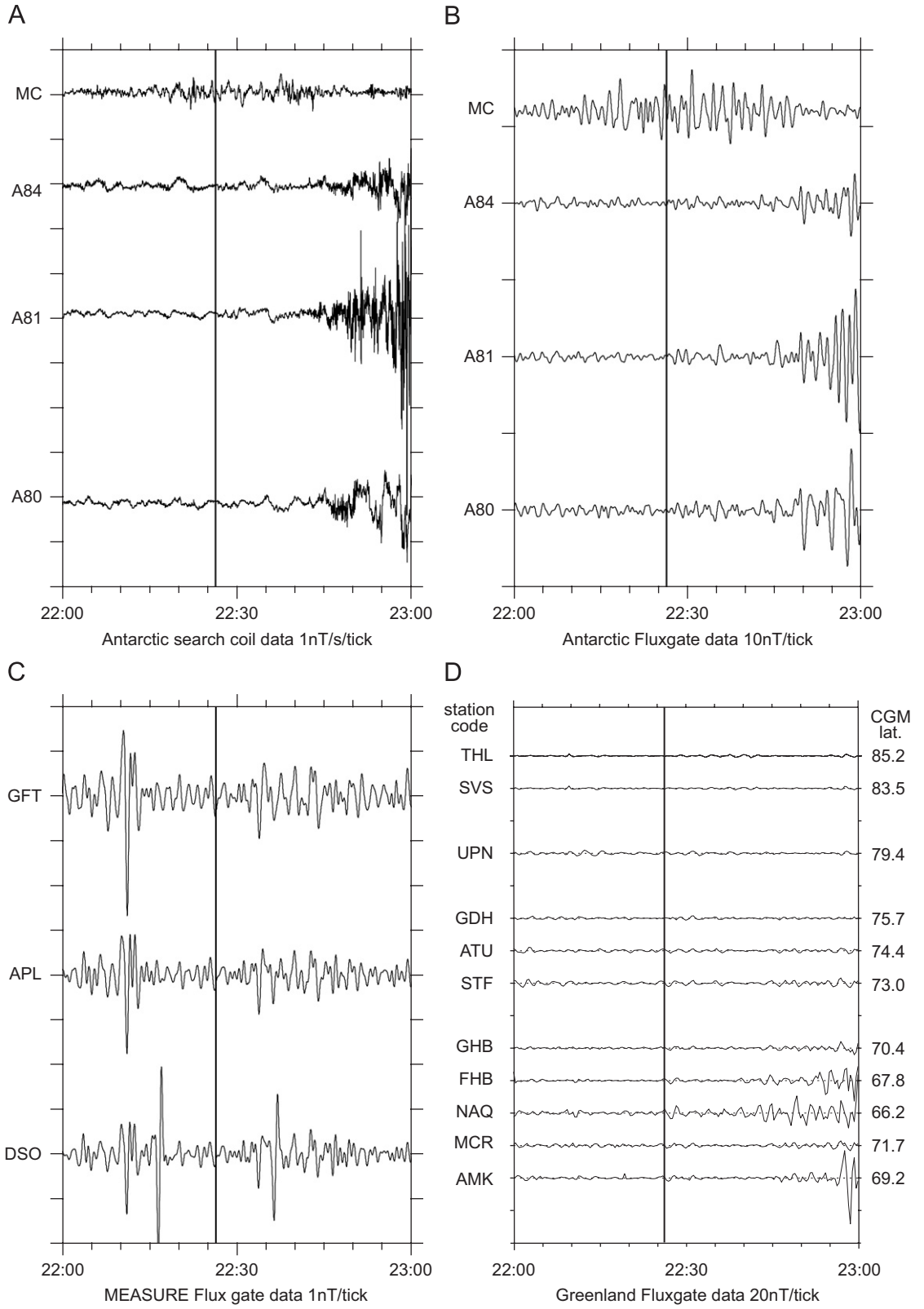

Fig. 9. Magnetometer data from several stations in Antarctica (A and B), North America (C), and Greenland (D) as in Fig. 3, but for January 23, 2001 (DOY = 023).

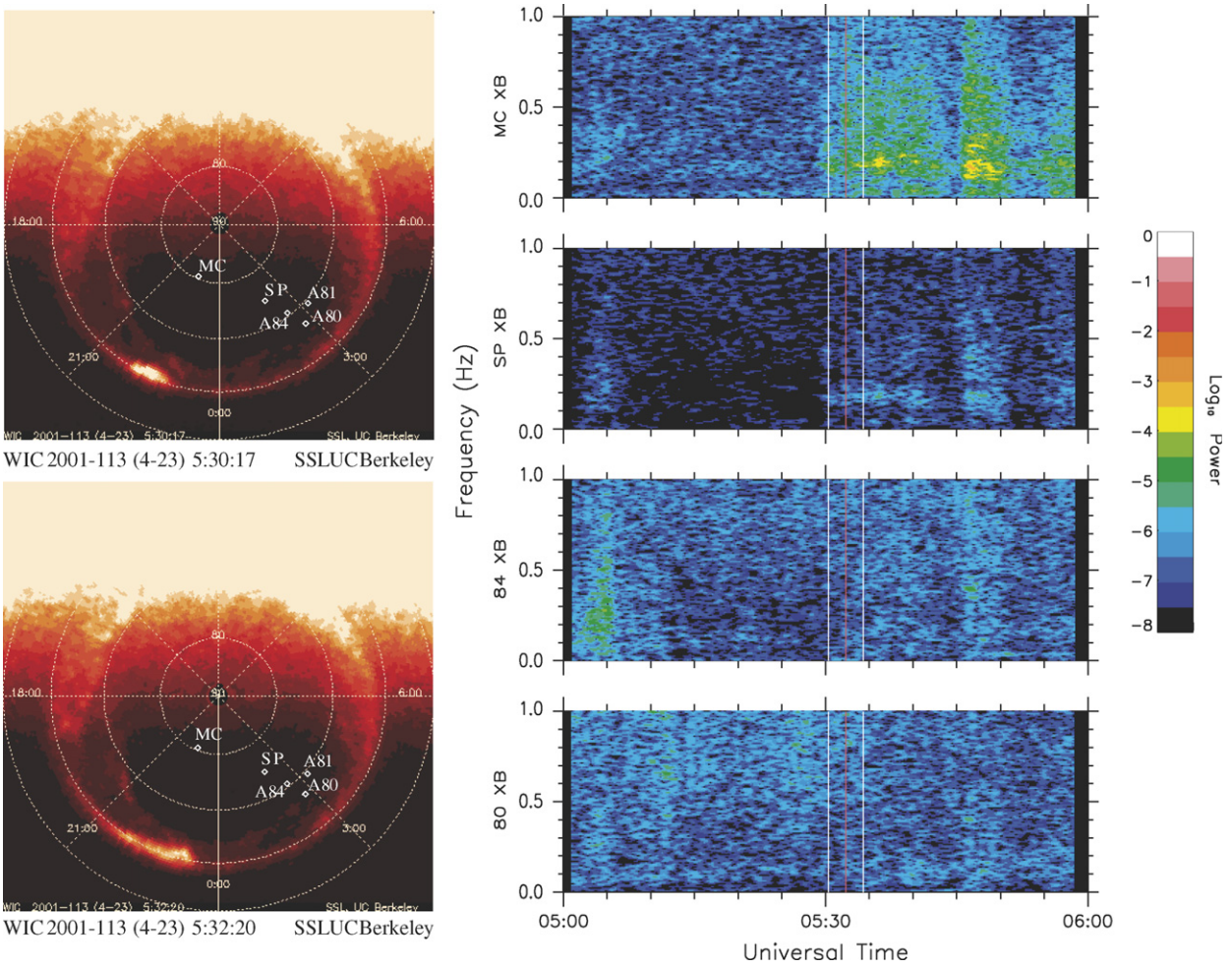

Fig. 10. The 2 panels on the left are the WIC images showing the substorm onset and the right side of the figure shows a 1-h, 0–1 Hz Fourier spectrogram of search coil data from several Antarctic ground stations as in Fig. 2, but for April 23, 2001 (DOY = 113).

substorm onset at any of the stations. The line plot of Antarctic search coil data (Fig. 9A) confirms that there was no evident Pi1B activity near substorm onset. Similarly, no Pi2 activity can be seen in the Antarctic fluxgate data shown in Fig. 9B or in the MEASURE fluxgate data shown in Fig. 9C. Possible Pi2 is only seen at the most equatorward Greenland site, NAQ (Fig. 9D).

3.2.2. April 23, 2001, substorm onset = 5:32:20 UT

The final example shown is for April 23, 2001 (DOY = 113). In this case, the WIC image shown in the lower left panel of Fig. 10 shows a weak substorm onset occurring at 5:32:20 UT with brightness = 7.1 kR. The substorm onset is located at 62.5° MLAT and 23.2 MLT. The stations are somewhat distant at ΔMLAT = 4.5 and ΔMLT = 3.4, but McMurdo is actually fairly close in MLT. No clear Pi1B activity can be seen at any of the auroral zone stations shown in the spectrogram in the right panel of Fig. 10. However, there is some evidence of weak continuous Pi activity (PiC) near 0.2 Hz at McMurdo and South Pole that begins within ±2 min of the onset time and continues intermittently for the next 30 min.

The 1-h time series of the Antarctic search coil magnetometer data (Fig. 11A) do not show any Pi1B activity. The faint PiC activity that was seen at South Pole and McMurdo in the spectrogram, however, is visible as a broadening of the traces at those stations. The fluxgate data from both the Antarctic and Greenland (Fig. 11B and D) does not show any clearly identifiable Pi2 activity. However, the MEASURE fluxgate data (Fig. 11C) show Pi2

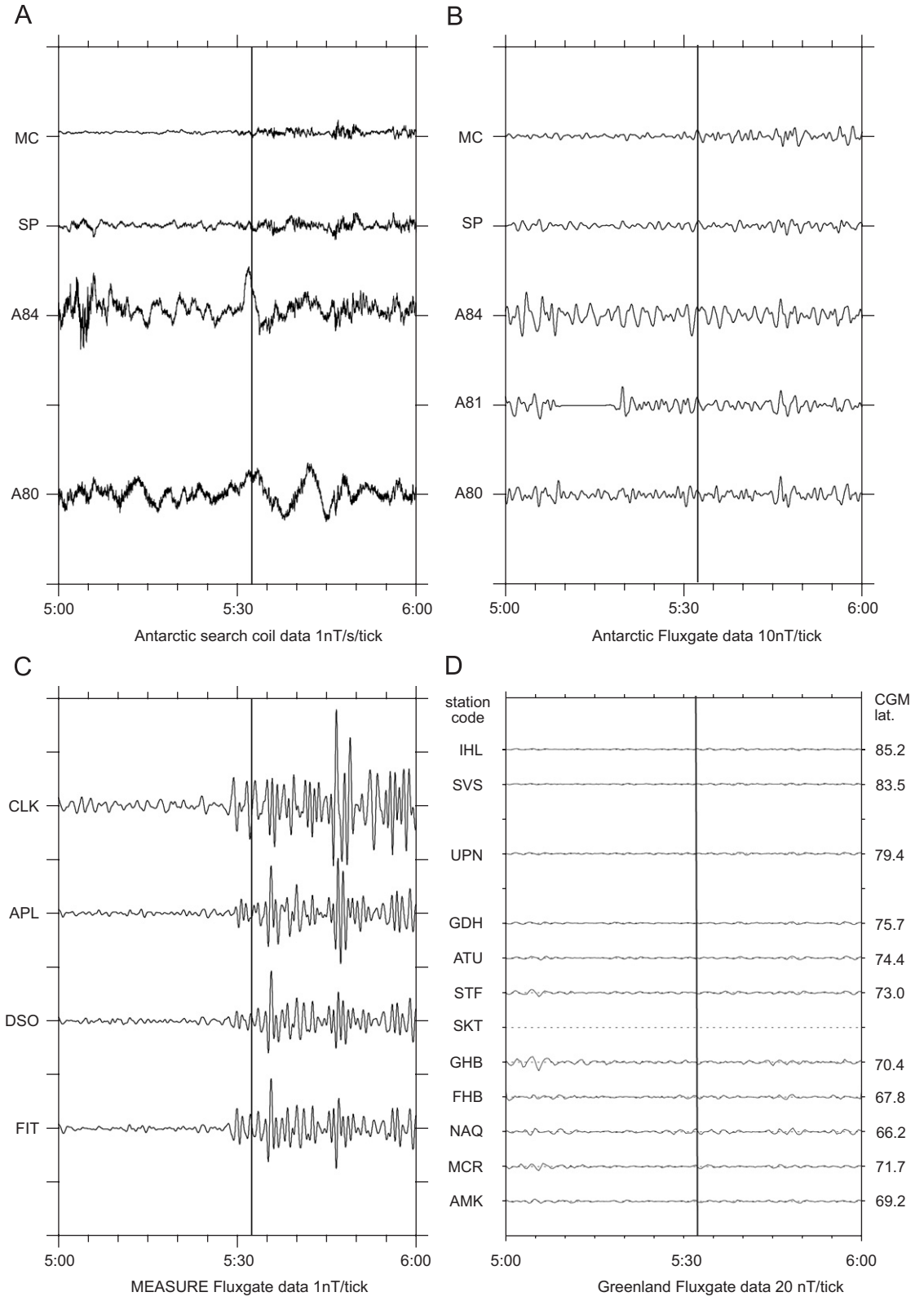

Fig. 11. Magnetometer data from several stations in Antarctica (A and B), North America (C), and Greenland (D) as in Fig. 3, but for April 23, 2001 (DOY = 113).

starting a few minutes before substorm onset, near 5:30 UT, which corresponds to an earlier brightening in the WIC image shown in the upper left panel of Fig. 10.

4. Statistical study

Spectrograms were inspected visually to look for Pi1B activity occurring near the time of substorm onset identified in the FUV-WIC imager data. Each event was classified in 1 of 5 categories: (1) Yes Strong (YesS), when clear Pi1B pulsations with power levels yellow or above on the color scale (10^{-4} nT^2 Hz or above) occurred at one or more stations within 0–2 min of the imager onset time; (2) Yes Weak (YesW), when clear Pi1B pulsations with power levels below yellow on the color scale (below 10^{-4} nT$^2 \times$ Hz) occurred at one or more stations within 0–2 min of the imager onset time; (3) No, when there were no visible Pi1B pulsations within 0–10 min of the imager onset time; (4) Questionable, when clear Pi1B pulsations of any power level occurred within 2–10 min of the imager onset; and (5) Questionable Weak, when Pi1B activity was too weak to be clearly identified within 0–2 min of substorm onset. Since the questionable events made up only 10% of the total events in both data sets and there was only 1 questionable weak event in each data set, we combined them for statistical purposes and refer to them as questionable all (?all).

Tables 2A and B include statistics for both sets of events: Table 2A the original list of 39 events and Table 2B the list of the 20 most intense events. The first 4 columns indicate the classification (YesS, YesW, No, ?all), the number of events in each classification, and the corresponding percentage. In the original 39 event set, YesS and No events were equal, occurring in 31% of the events. YesW events occurred in 26% of the original 39 events and ?all in 13%. In the 20 most intense events list, YesS events occurred most often, 45%, and the YesW and no events fell to only 20% each. The ?all events occurred in 15% of the events, similar to their occurrence in the original 39 event set. The average brightness for each classification is shown in column 4. In both lists, the YesS events have the largest values of average brightness; the YesW, No, and ?all events were about equal and about 3–5 kR less intense than the YesS values.

Table 2A
Statistical results for the original 39 events

	Number	Percent	Average		
			Brightness (kR)	|ΔMLAT| (deg)	|ΔMLT| (h)
YesS	12	31	13.6	2.4	1.6
YesW	10	26	8.5	3.2	2.3
No	12	31	8.8	3.7	4.2
?all	5	13	9.0	4.4	2.3

Table 2B
Statistical results for the 20 most intense events

	Number	Percent	Average		
			Brightness (kR)	|ΔMLAT| (deg)	|ΔMLT| (h)
YesS	9	45	23.6	3.1	2.6
YesW	4	20	20.5	4.1	3.8
No	4	20	18.3	3.0	5.9
?all	3	15	18.0	5.4	5.2

Columns 5 and 6 show the averages of the |ΔMLAT|, defined as the absolute value of difference in degrees between the onset location identified in the WIC imager data and the reference latitude of the auroral zone stations used in this study, and |ΔMLT|, defined as the absolute value of the difference in hours between the onset location identified in the WIC imager data and the reference local time of the auroral zone stations used in this study. The location of the substorm onset, given to two decimal places, is defined by the position of the most intense pixel in the substorm surge (Frey et al., 2004). Accuracy to 1 decimal place is used for analysis in this study.

In the original 39 event set, the average |ΔMLT| was smallest for the YesS category (1.6 h), increased to 2.3 h for the YesW category, and was largest for the No category (4.2 h). The average |ΔMLAT| for these events followed a similar pattern, with the YesS, YesW, and No categories having values of 2.4°, 3.2°, and 3.7°, respectively. The average |ΔMLT| for the 20 intense events was similar to that of the original 39, but the values were slightly higher for each of the categories, YesS, YesW, and No. The average |ΔMLAT| for these events was somewhat different; the YesS and No categories both had an average |ΔMLAT| of about 3° and the YesW category had a value near 4°.

Figs. 12A and B show the number of events vs. magnetic local time for the 39 original events and

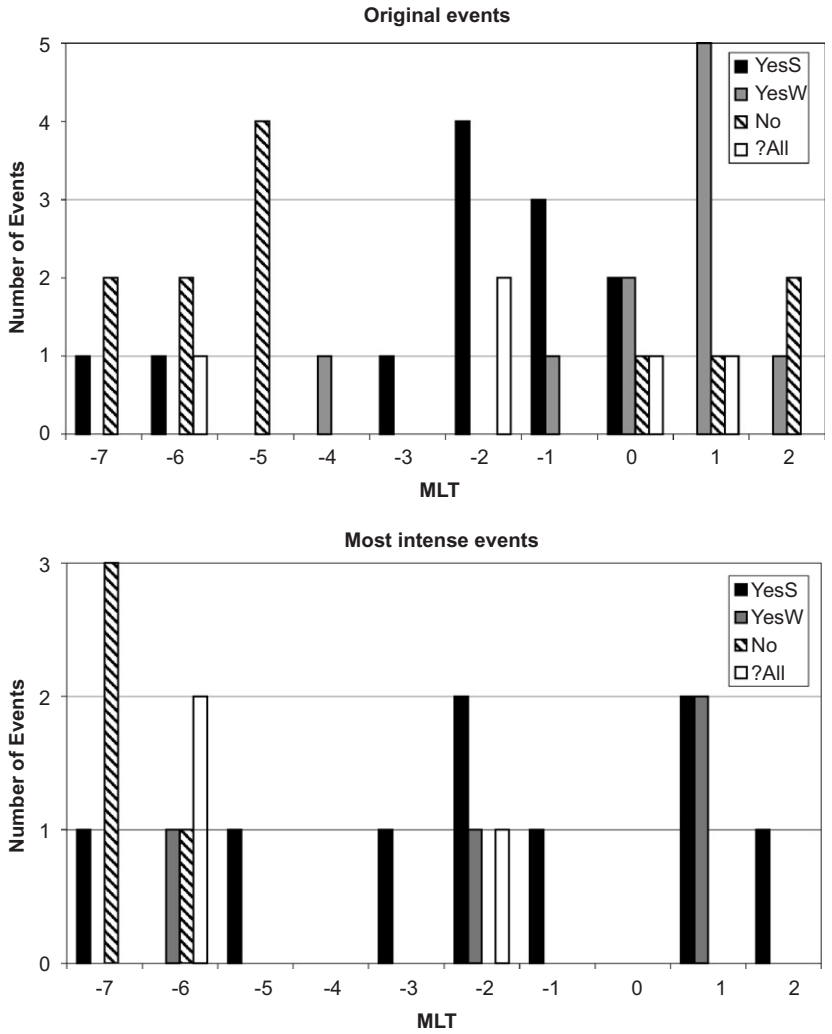

Fig. 12. Distribution of events as a function of magnetic local time for the 39 original events (upper panel) and the 20 most intense events (lower panel. Black indicates Yes/strong events, gray Yes/weak events, diagonal fill No events, and white questionable (?) events).

for the 20 most intense events. The YesS events, represented as black, and YesW, represented as gray, occurred predominantly when the ground stations were between −3 and 2 MLT for all storm intensities. The No events occurred most often when the onset was 5 h or more prior to local midnight.

5. Limiting factors

Fig. 13 shows the dependence of Pi1B activity occurrence on brightness, ΔMLAT, and ΔMLT. Each of the panels of Fig. 13 show YesS (solid circle),YesW (open circle) and No (X) events from both lists divided into 4 groups based on the brightness and then plotted as a function of ΔMLAT and ΔMLT.

For the most intense events, with brightness greater than 16.3 kR, YesS and YesW events occurred out to ± 5ΔMLT and the ΔMLAT did not limit these intense events. All 4 No events occurred when the stations were duskward of the onset location and more than 4 h away in MLT.

For the events with brightness less than 16.3 kR, the YesS and YesW events occurred most often when ΔMLT was within ± 2 and ± 4 h, respectively. For the events with lower intensity, a larger ΔMLAT played a more important role in limiting the occurrence of Pi1B than in the more intense events.

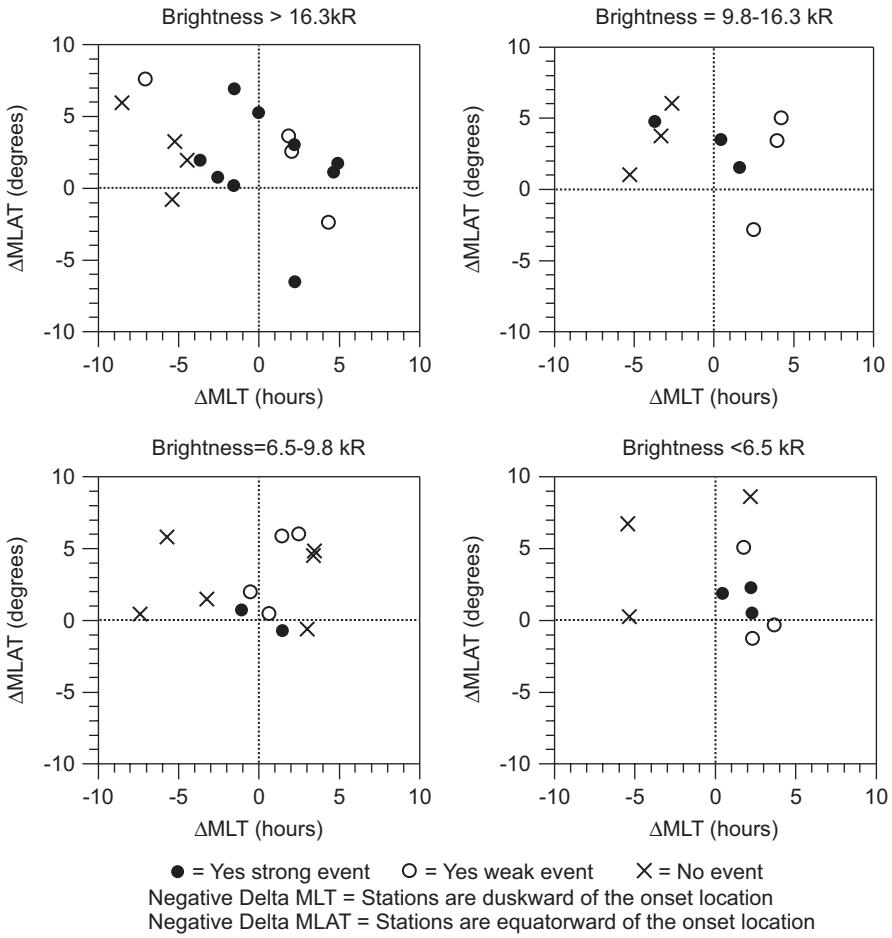

Fig. 13. ΔMLAT vs. ΔMLT for all events divided into four groups based on the intensity of the auroral image (brightness). The upper left graph shows events greater than 16.3, the upper right events 9.8–16.3 kR, the lower left events 6.5–9.8 kR, and the lower right events less than 6.5 kR. Yes/strong events are indicated by solid circles, Yes/weak by open circles and No events by an X. Negative ΔMLT indicates that the stations are duskward of the onset location and negative ΔMLAT indicates that the stations are equatorward of the onset location.

6. Discussion

Both the statistical study above and individual examples have documented good temporal agreement between the appearance of Pi1B signatures in ground magnetometer data and the onset times of substorm events identified by the IMAGE satellite. The examples of substorm onsets with Pi1B activity above also show that the amplitude of Pi1B signals weakens as the observing site becomes more distant from the footpoint of the substorm onset, and may not be seen at all at the most distant stations. Because of the limited range of Pi1B signatures in both magnetic local time and magnetic latitude, Pi1B can provide information about onset location as well as onset time.

Tables 3A and B show the number of events as a function of |ΔMLT|, the distance between the substorm onset location as determined from the WIC images and the reference location of the Antarctic auroral ground stations. It is apparent from Tables 3A and B that a large majority of substorm onsets observed within 2 h MLT of the ground sites were correlated in time with a Pi1B event (YesS or YesW): 76% for the original set of 39 and 88% for the set of the most intense events. Pi1B activity is thus strongly localized in local time near substorm onset. Significantly, the single No event that occurred within 2 h MLT was over 8° MLAT away from the reference location of the search coil sites and was also weak, with brightness = 5.3 kR.

Table 3A
Number of Pi1B events in each of 4 categories as a function of ΔMLT for the original 39 events

Original39	ΔMLT				
	⩽1	2	3	4	⩾5
YesS	5	5	1	1	0
YesW	3	3	1	3	0
No	0	1	6	0	5
?all	3	1	0	0	1

Table 3B
Number of Pi1B events in each of 4 categories as a function of ΔMLT for the 20 most intense events

20 intense	ΔMLT				
	⩽1	2	3	4	⩾5
YesS	1	4	1	1	2
YesW	0	2	0	1	1
No	0	0	0	1	3
?all	1	0	0	0	2

These distributions of spatial extent are consistent with the earlier studies of auroral zone Pi1B and Pi2 by Parkhomov and Rakhmatulin (1975), Parkhomov et al. (1976), and Rakhmatulin et al. (1979). Their finding that the spatial extent of Pi1B events was about 5° in latitude is consistent with the latitudinal distributions shown in Fig. 13, which indicate that only the brightest auroral onsets could be associated with Pi1B observations more than 5° away in MLAT. Similarly, their finding that the longitudinal extent of Pi1B was less than 30° (2 h MLT) is consistent with the longitudinal distributions shown in Fig. 13, which again indicates that in almost all cases, only the brightest auroral onsets could be associated with Pi1B observations more than 2 h away in MLT. These studies also noted that the longitudinal extent of Pi2 ranged from 30° to 120° (2–8 h MLT), again much larger than that for Pi1B.

Sutcliffe (1980) indicated that range over which Pi2 pulsations at low latitudes can be observed changes from substorm to substorm, ranging from only 1–2 h MLT in some cases to the entire nightside hemisphere. However, the extent of the range was found not to be a function of substorm intensity. This variability is consistent with the lack of proportionality between the amplitude of Pi2 signatures in MEASURE data and the observed UV brightness noted in Section 3.1.2.

For completeness, we study further the 5 questionable Pi1B events that also occurred within 2 h MLT. Three of those questionable events of various intensities occurred over 8° MLAT away. This is consistent with the fact that there were no YesS or YesW events that occurred with ΔMLAT ⩾8°. The other 2 questionable events were close in both ΔMLAT and ΔMLT and had intensities of ~7.0 kR. These events had clear Pi1B signatures that occurred about 4 min after the substorm onset. Analysis of all available WIC images between the onset time and the time of the Pi1B activity showed that a second substorm brightening occurred at the time of the Pi1B activity almost directly over some of the Antarctic ground stations. This second brightening was not listed as an event most likely because it occurred too close in time to the initial substorm onset. Frey et al. (2004) indicated that an onset was only accepted as a separate event if at least 30 min had passed after the previous onset. This secondary brightening may explain why Pi1B activity appeared at these sites at a different time but it does not explain why no Pi1B appeared coincident with the initial substorm onset.

Another possibility to explain these events is the effect of the clock angle causing auroral asymmetries between the hemispheres. In both of the questionable cases described above where the auroral brightening appeared to be close to the Antarctic stations, the clock angle caused the location of the auroral brightening to be shifted dawnward by ~1.3 and ~1.5 h in MLT, bringing the auroral brightening even closer in MLT. In the 3 Yes events described above (in Section 3.1), the shift in MLT of the auroral brightening locations was in each case less than 0.5 h and was therefore not analyzed further. Another point not yet understood is that Pi1B activity sometimes was observed when the substorm onset was ⩾3 h away in MLT from the reference auroral zone station location. This can be partially explained by the intensity of the substorm, since there were 2 YesS events in the ⩾5 ΔMLT classification for the 20 most intense events and none for the original 39.

In order to provide a quantitative estimate of the falloff of Pi1B signals at the time of substorm onset with distance, we have plotted in Fig. 14 an estimate of the observed Pi1B amplitude at each station near the time of substorm onset vs. great circle distance in kilometers between each station to the brightest point of the substorm onset location, using a log-log scale, for the 3 example Yes events described in Section 3.1. The dashed line near the bottom of this

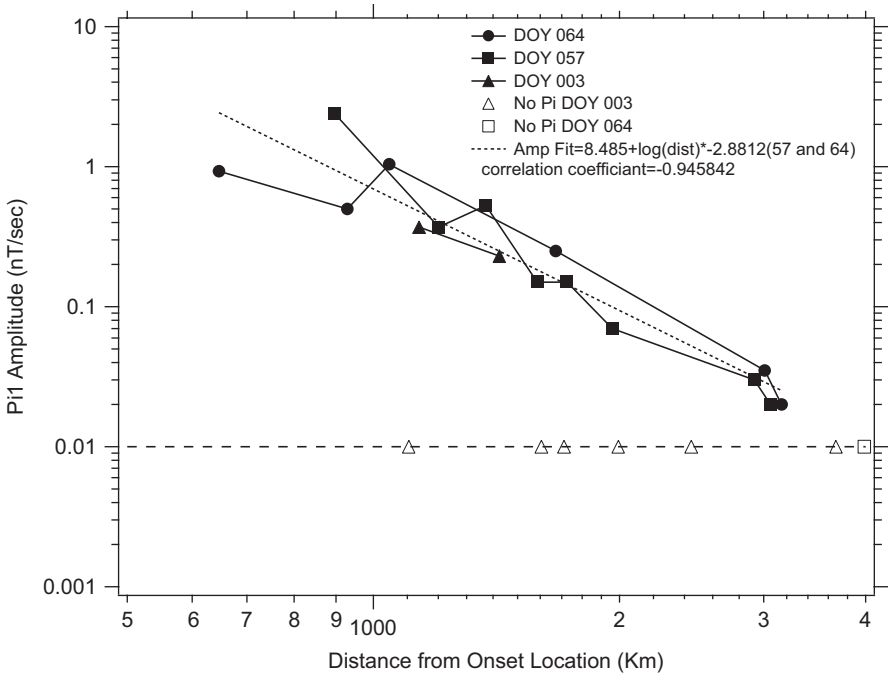

Fig. 14. Pi1B amplitude at the time of substorm onset vs. distance from onset location for the three Yes events described in Section 3.1.

figure represents the estimated minimum amplitude threshold for detecting Pi1B activity. The open symbols along this line indicate the distances of stations where data were available but did not show any indication of detectable Pi 1 activity. A distance of 1000 km on the horizontal scale corresponds to approximately 9° in MLAT. A distance of 1000 km in longitude at 67° MLAT is about 23° in longitude or 1.5 h MLT and at 74° MLAT is about 33° in longitude or 2.2 h MLT.

The dotted line in Fig. 14 is a linear least-squares fit to the observations for days 057 and 064. The slope of this line thus indicates that Pi1B amplitude falls off as distance$^{-2.9}$ with a correlation coefficient of −0.95, i.e., similar to the r^{-3} falloff of the signal from a dipolar source. Using this best-fit line, a doubling of the distance corresponds roughly to a decrease of a factor of 7.5 in amplitude. Similar analysis of Pi2 pulsations for the same days indicates an amplitude fall off as distance$^{-2.8}$ with a correlation coefficient of −0.93.

Although the falloff of Pi1B power with distance for these 2 events appears to be quite consistent, the uncertainty in determining especially the lower amplitudes is substantial; we estimate it to be approximately a factor of 2. The Pi1B signals for the event of January 3, 2001, however, were much more highly localized, appearing only at A80 and A81. No detectable Pi1B activity was observed at the remaining stations, thus making a power law fit for the signals on this day not physically valid. Similarly, Pi2 signals on this day were clear at A80, A81, and SP, but not at the other Antarctic stations. However, as noted in Section 3.1.2, the Pi2 signals observed by the MEASURE array were actually stronger on this day than on day 057. The observations presented here thus show the unexpected complexity of the Pi1B and Pi2 magnetic signatures associated with substorm onsets. Although additional studies will certainly be necessary to determine whether the above examples are representative, it appears that during strong events Pi1B signals fall off slightly more rapidly than Pi2 signals, and that during weaker events Pi1B signals may be highly localized, with possibly asymmetric falloffs in latitude and longitude.

7. Conclusions

We have used simultaneous satellite-based UV imager data and ground-based search coil magnetometer data to investigate the spatial extent of Pi1B signatures of substorm onsets. Based on the examples shown and our statistical observations, we have shown the following:

1. Within the cadence of the IMAGE FUV images (2 min), Pi1B onsets occur simultaneously with intense isolated auroral substorms.
2. Most events are observed to occur between 2100 and 0200 MLT. This non-global characteristic implies that the mechanism that drives Pi1B pulsations is likely different than that driving Pi2 pulsations.
3. Observations are quite localized, with the strongest events limited to $\pm 5^{\circ}$ in MLAT and ± 2 h in MLT, consistent with the few published results from earlier studies.
4. The amplitude dependence on distance falls of as r^{-3}, based on a power law fit to 2 strong events. A more rapid falloff was noted with a weaker event. This is similar to that of high-latitude Pi2 signals, but different from mid-latitude Pi2 signals, which tend to drop off much more slowly.

Further analysis of the spatial falloff of Pi1B activity with distance is currently limited by the small number of search coil arrays in operation. The observations reported here, however, do suggest that monitoring of Pi1B activity from a dense spatial array of magnetometers sensitive to 0.1–1 Hz activity (both search coil and low-noise fluxgate instruments) may provide improved information on onset location (and potentially on timing) that can thus contribute to substorm studies, especially in the absence of satellite imager data.

We note finally that Pi1B signals contain polarization information as well as amplitude and timing data. A more complete analysis of the vector signals is in progress to evaluate the possibility that Pi1B signals from a suitably located array of ground stations might be able to provide even more detailed information on the location of substorm onsets via polarization analysis and triangulation. Even without this latter potential application, we expect that the combined ground and satellite observing systems to be deployed for the THEMIS project later this decade will provide the means to further test the usefulness of these transient magnetic signals for substorm studies.

Acknowledgments

We thank V.A. Pilipenko for helpful comments and criticisms. Search coil magnetometer observations were supported by National Science Foundation Grants OPP-0341512, ANT-0442648, and OPP-0538379 to Augsburg College, and by Grants ANT-0442787, ANT-0520475 and ANT-0538474 to the University of New Hampshire. The IMAGE FUV investigation was supported by NASA through SwRI Subcontract 83820 at the University of California at Berkeley under Contract NAS5-96020. The fluxgate magnetometers at South Pole and McMurdo are supported at Siena College and NJIT by NSF OPP-338105, and the AGO fluxgate magnetometers at Siena College and NJIT by NSF OPP-0341046. Grant support for MEASURE is from the National Science foundation under Grant ATM-0196223. We acknowledge the assistance of the US Antarctic Program in supporting the operation of the magnetometers at South Pole Station and the US AGOs, and of the British Antarctic Survey in supporting the operation of the magnetometers at the BAS AGOs.

References

Arnoldy, R.L., Posch, J.L., Engebretson, M.J., Fukunishi, H., Singer, H.J., Onsager, T., 1998. Pi1 magnetic pulsations in space and at high latitudes on the ground. Journal of Geophysical Research 103, 23581–23591.

Dudeney, J.R., Horne, R.B., Jarvis, M.J., Kressman, R.I., Rodger, A.S., Smith, A.J., 1997. British Antarctic Survey's ground-based activities complementary to satellite missions such as cluster. In: Lockwood, M., Wild, M.N., Opgenoorth, H.J. (Eds.), Satellite-Ground Based Coordination Sourcebook, ESA-SP-1198. ESA Publications, ESTEC, Noordwijk, The Netherlands, pp. 101–109.

Engebretson, M.J., et al., 1997. In: Lockwood, M., Wild, M.N., Opgenoorth, H.J. (Eds.), Satellite–Ground Based Coordination Sourcebook, ESA-SP-1198. ESA Publications, ESTEC, Noordwijk, The Netherlands, pp. 65–99.

Frey, H.U., Mende, S.B., Immel, T.J., Gerard, J.-C., Hubert, B., Habraken, S., Spann, J., Gladstone, G.R., Bisikalo, D.V., Shematovich, V.I., 2003. Summary of quantitative interpretation of IMAGE far ultraviolet auroral data. Space Science Reviews 109, 255–283.

Frey, H.U., Mende, S.B., Angelopoulos, V., Donovan, E.F., 2004. Substorm onset observations by IMAGE-FUV. Journal of Geophysical Research 109, A10304.

Keiling, A., Fujimoto, M., Hasegawa, H., Honary, F., Sergeev, V., Semenov, V.S., Frey, H.U., Réme, H., Dandouras, I., Lucek, E., 2006. Association of Pi2 pulsations, auroral breakup and pulsed reconnection: ground and cluster observations in the tail lobe at 16 Re. Annales Geophysicae 24, 3433–3449.

Kepko, L., Kivelson, M.G., 1999. Generation of Pi2 pulsations by bursty bulk flows. Journal of Geophysical Research 104, 25,021–25,034.

Kepko, L., Kivelson, M.G., Yumoto, K., 2001. Flow bursts, braking and Pi2 pulsations. Journal of Geophysical Research 106, 1903–1916.

Kim, K.-H., Lee, D.-H., Denton, R.-E., Takahashi, K., Goldstein, J., Moon, Y.-J., Yumoto, K., Pyo, Y.S., Keiling, A.,

2005. Pi2 pulsations in a small and strongly asymmetric plasmasphere. Journal of Geophysical Research 110, A10201.

Lessard, M.R., Lund, E.J., Jones, S.L., Arnoldy, R.L., Posch, J.L., Engebretson, M.J., Hayashi, K., 2006. The nature of Pi1B pulsations as inferred from ground and satellite observations. Geophysical Research Letters 33, 14108.

Mende, S.B., et al., 2000. Far ultraviolet imaging from the IMAGE spacecraft. Space Science Reviews 91, 287.

Olson, J.V., 1999. Pi2 pulsations and substorm onsets: a review. Journal of Geophysical Research 104, 17499–17520.

Olson, J.V., Rostoker, G., 1978. Pi 2 pulsations and the auroral electrojet. Planetary and Space Science 23, 1129–1139.

Østgaard, N., Mende, S.B., Frey, H.U., Immel, T.J., Frank, L.A., Sigwarth, J.B., Stubbs, T.J., 2004. Interplanetary magnetic field control of the location of substorm onset and auroral features in the conjugate hemispheres. Journal of Geophysical Research 109, A07204.

Østgaard, N., Tsyganenko, N.A., Mende, S.B., Frey, H.U., Immel, T.J., Fillingim, M., Frank, L.A., Sigwarth, J.B., 2005. Observations and model predictions of substorm auroral asymmetries in the conjugate hemispheres. Geophysical Research Letters 32, L05111.

Parkhomov, V.A., Rakhmatulin, R.A., 1975. Localization and Drift of Pi1B Source (Issledovaniya po geomagnetizmu, aeronomii i fizike Solntsa), Vol. 36. Nauka, Moscow, pp. 131–137 (in Russian).

Parkhomov, V.A., Rakhmatulin, R.A., Solovjev, S.J., Polyushkina, T.N., Barkova, L.M., 1976. The Azimuthal Drift of Pi1B Source (Issledovaniya po geomagnetizmu, aeronomii i fizike Solntsa), Vol. 39. Nauka, Moscow, pp. 33–37 (in Russian).

Rakhmatulin, R.A., Parkhomov, V.A., Vakulin, Y.I., 1979. The Dynamics of Auroral Electrojet and Irregular Pulsations During Substorm Breakup Phase (Issledovaniya po geomagnetizmu, aeronomii i fizike Solntsa), Vol. 46. Nauka, Moscow, pp. 89–94 (in Russian).

Rosenberg, T.J., Doolittle, J.H., 1994. Studying the polar ionosphere and magnetosphere with Automatic Geophysical Observatories: the United States program in Antarctica. Antarctic Journal of the United States 29 (5), 347.

Rostoker, G., Olson, J.V., 1978. Pi 2 micropulsations as indicators of substorm onsets and intensifications. Journal of Geomagnetism and Geoelectricity 30, 135–147.

Sutcliffe, P.R., 1980. The longitudinal range of Pi2 propogation at low latitudes. Planetary and Space Science 28, 9–16.

Takahashi, K., Ohtani, S.-I., Hughes, W.J., Anderson, R.R., 2001. CRRES observation of Pi2 pulsations: wave mode inside and outside the plasmasphere. Journal of Geophysical Research 106, 15,567.

Taylor, W.W.L., Parady, B.K., Lewis, P.B., Arnoldy, R.L., Cahill Jr., L.J., 1975. Initial results from the search coil magnetometer at Siple, Antarctica. Journal of Geophysical Research 80, 4762–4769.